ChemComm

COMMUNICATION

View Article Online
View Journal | View Issue

Cite this: *Chem. Commun.*, 2021, 57, 6640

Received 31st March 2021,
Accepted 20th May 2021

DOI: 10.1039/d1cc01716k

rsc.li/chemcomm

Distinct photodynamics of κ-N and κ-C pseudoisomeric iron(II) complexes†‡

Philipp Dierks,[a] Ayla Kruse,[b] Olga S. Bokareva,[bc] Mohammed J. Al-Marri,[bd] Jens Kalmbach,[e] Marc Baltrun,[a] Adam Neuba,[a] Roland Schoch,[a] Stephan Hohloch,[f] Katja Heinze,[g] Michael Seitz,[e] Oliver Kühn,[b] Stefan Lochbrunner[b] and Matthias Bauer*[a]

Two closely related Fe^{II} complexes with 2,6-bis(1-ethyl-1*H*-1,2,3-triazol-4yl)pyridine and 2,6-bis(1,2,3-triazol-5-ylidene)pyridine ligands are presented to gain new insights into the photophysics of bis(tridentate) iron(II) complexes. The $[Fe(N^N^N)_2]^{2+}$ pseudoisomer sensitizes singlet oxygen through a MC state with nanosecond lifetime after MLCT excitation, while the bis(tridentate) $[Fe(C^N^C)_2]^{2+}$ pseudoisomer possesses a similar ^{3}MLCT lifetime as the tris(bidentate) $[Fe(C^C)_2(N^N)]^{2+}$ complexes with four mesoionic carbenes.

Utilization of solar energy is a current scientific challenge. Light harvesting approaches based on d^6 metal complexes of Ru^{II}, Os^{II} and Ir^{III} with π-accepting ligands have been widely explored.[1] The search for earth-abundant alternatives focusses on iron complexes.[2,3] Challenge here is the small ligand field splitting, leading to short-lived MLCT (Metal to Ligand Charge Transfer) states due to MC (Metal Centred) states of lower energy. Several strategies are available to extend the MLCT lifetimes of iron complexes. The ligand field splitting can be increased by strong σ-donors like N-heterocyclic carbenes (NHCs)[4] or optimization of the octahedral symmetry.[5,6] MLCT states can be stabilized by π-acceptor ligands or increased excited electron delocalization.[7] Following these strategies, MLCT lifetimes could be increased from 0.15 ps in $[Fe(tpy)_2]^{2+}$ (tpy = 2,2′:6′,2″-terpyridine) over 9 ps in $[Fe(bim)_2]^{2+}$ (bim = 2,6-bis(imidazol-2-ylidene)pyridine)[8] to 528 ps in $[Fe(btz)_3]^{2+}$ (btz = 4,4′-bis(1,2,3-triazol-5-ylidene)).[9] Polypyridyl ligands are weak σ-donors, but good π-acceptors. In contrast, carbenes in $[Fe(bim)_2]^{2+}$ are stronger σ-donors and weaker π-acceptors. Mesoionic carbenes (MICs) like in $[Fe(btz)_3]^{2+}$ are both strong σ-donors and moderate π-acceptors.[10–12] For NHC–iron(II)-complexes, the lifetime of ^{3}MLCT states has shown to increase with the number of NHC and MIC units.[9,13,14]

Since triazolylidenes as a special class of MICs, can be synthesized *via* methylation of the corresponding triazoles, they offer a unique possibility to address some fundamental questions in the photochemistry of Fe^{II} complexes using tridentate ligands. Such complexes usually offer higher chemical stability, but lower octahedral symmetry compared to Fe^{II} complexes of bidentate ligands. Although Fe^{II} triazole complexes are known for their spin-crossover properties[15,16] their photophysics are unexplored. Moving from the triazole Fe^{II} complex **Fe1** to the MIC complex **Fe2** (Scheme 1) allows to address how much the degree of octahedral symmetry – in the sense of the C–Fe–C *trans* angle – affects the excited state landscape by comparison of bis(tridentate) with tris(bidentate) MIC complexes. Therefore two new Fe^{II} complexes with 2,6-bis(1-ethyl-1*H*-1,2,3-triazol-4-yl)pyridine (**2**) **Fe1** and 2,6-bis(1,2,3-triazol-5-ylidene)pyridine (**3**) ligand **Fe2** as a bis(tridentate) tetra-MIC type were prepared (Scheme 1). **2** is obtained by coupling of 2,6-dibromopyridine with trimethylsilylacetylene to give **1** and a azide–alkyne cyclization of **1** with *in situ* prepared ethylazide. Triazole **2** is methylated with methyltriflate in DCM at −80 °C to give the triazolium salt **3**. Reaction of $FeBr_2$ in degassed ethanol with **2** yields **Fe1**. The preparation of **Fe2** requires deprotonation of **3** with LiHMDS in THF at −80 °C and addition of $FeBr_2$.

The key structural parameters obtained from single crystal diffraction are discussed by comparing **Fe1** to $[Fe(tpy)_2]^{2+}$ as

[a] *Faculty of Science, Chemistry Department and Centre for Sustainable Systems Design, Paderborn University, 33098 Paderborn, Germany. E-mail: matthias.bauer@upb.de*
[b] *Institute of Physics and Department of Life, Light and Matter, University of Rostock, 18051 Rostock, Germany*
[c] *Department of Physical Chemistry, Kazan Federal University, 420008 Kazan, Russia*
[d] *College of Engineering, Qatar University, P.O. Box 2713, Doha, Qatar*
[e] *Institute of Inorganic Chemistry, University of Tübingen, Auf der Morgenstelle 18, 72076 Tübingen, Germany*
[f] *University of Innsbruck, Faculty of Chemistry and Pharmacy, Institute for General, Inorganic and Theoretical Chemistry, Innrain 80-82, Innsbruck 6020, Austria*
[g] *Department of Chemistry, Johannes Gutenberg, University of Mainz, 55128 Mainz, Germany*

† Dedicated to the memory of Prof. Dr Markus Gerhards.

‡ Electronic supplementary information (ESI) available: Synthetic procedures, NMR spectra, MS data, crystallographic data, information on computational studies, experimental details of the transient absorption and $^1O_2$ sensitization experiments. CCDC 2049729 and 2050317. For ESI and crystallographic data in CIF or other electronic format see DOI: 10.1039/d1cc01716k

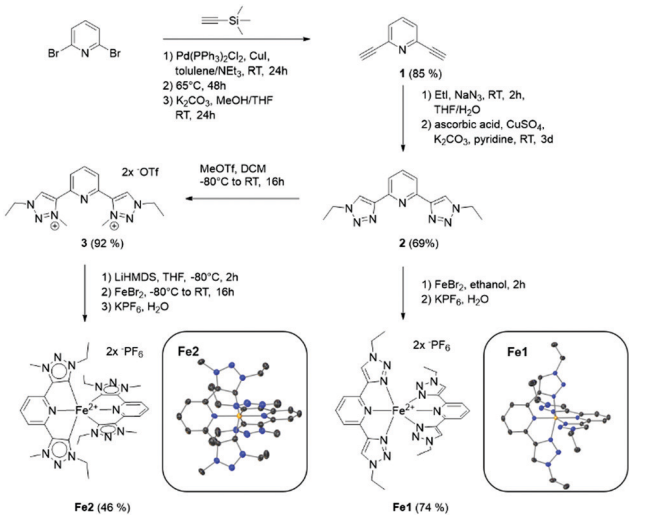

Scheme 1 Syntheses of **Fe1** and **Fe2** with corresponding single crystal structures shown in insets.

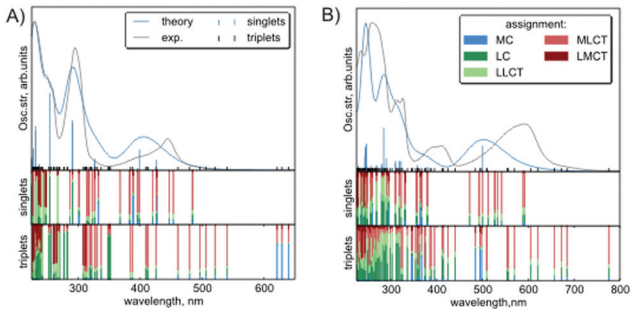

Fig. 1 Experimental and theoretical absorption spectra of **Fe1** (panel A, upper part) and **Fe2** (panel B, upper part) as well as density-matrix analysis[21] based assignment of corresponding vertical singlet and triplet excited states (lower parts). Broadening of theoretical spectra is done by Gaussian function (FWHM 0.2 eV). The legends in panel (A) are also valid for panel (B) and *vice versa*.

$[Fe(N^N^N)_2]^{2+}$ reference. **Fe2** is compared to $[Fe(bim)_2]^{2+}$ and $[Fe(btz)_2(bpy)]^{2+}$ as bis(tridentate) $[Fe(C^N^C)_2]^{2+}$ and tris (bidentate) $[Fe(C^C)_2(N^N)]^{2+}$ reference. The Fe–N bond length of 1.9539(9) Å in **Fe1** and the N–Fe–N *trans* angle of 161.06(4)° are only slightly changed with respect to 1.987(3) Å and 161.55(12)° in $[Fe(tpy)_2]^{2+}$.[17] Thus, the different electronic properties of the triazole and tpy ligands only slightly affect the crystal structure. A different picture can be found for **Fe2** in comparison to the bis(tridentate) $[Fe(bim)_2]^{2+}$. The C–Fe–C *trans* angle of 159.68(17)° in **Fe2** indicates an increased octahedral symmetry in comparison to 158.32(15)° in $[Fe(bim)_2]^{2+}$. The $Fe–N_{pyridine}$ bond length is elongated from 1.925(3) Å in $[Fe(bim)_2]^{2+}$ to 1.956(3) Å in **Fe2** by stronger π-backdonation. This interpretation is confirmed by the shortening of the $Fe–C_{carbene}$ bond length from 1.9665(3) Å in $[Fe(bim)_2]^{2+}$ to 1.9403(4) Å in **Fe2**.[8] The structural parameters, which are in line with those of $[Fe(btp)_2]^{2+}$ reported by Iwasaki *et al.*[18] (btp = 2,6-bis(1-mesityl-2,3-triazol-5-ylidene)pyridine), therefore support the stronger σ-donating character of MICs in comparison to classical NHCs. Bidentate ligands are advantageous to achieve a high octahedral symmetry. Accordingly, the tris(bidentate) tetra-MIC complex $[Fe(btz)_2(bpy)]^{2+}$ – with the same number of MIC and N-donors as **Fe2** – shows a much larger C–Fe–C *trans* angle of 173.0(7)° when compared to 159.68(17)° in **Fe2**. Although the strong σ-donating character of MICs is also reflected in the comparatively short $Fe–C_{carbene}$ bond length of 1.967(17) Å in $[Fe(btz)_2(bpy)]^{2+}$, this value is also shorter in the bis(tridentate) complex **Fe2**.

The optical absorption spectra of **Fe1** and **Fe2** together with TDDFT calculations with an optimally-tuned range-separated LC-BLYP functional are shown in Fig. 1.[7,19–21] The intense bands below 350 nm are dominated by ligand π–π* transitions. The presence of small intensity MLCT transitions in this region should be noted. At 444 nm, **Fe1** exhibits a sharp absorption maximum with an additional shoulder at higher energies. These features are assigned to MLCT transitions with some admixture of MC character, which is also known for $[Fe(tpy)_2]^{2+}$.[13] **Fe2** shows a much broader MLCT absorption. The lowest energy maximum is at 593 nm and thus lower in energy than in $[Fe(bim)_2]^{2+}$.[13] **Fe2** shows a MLCT shift from 593 nm to 609 nm in comparison to $[Fe(btz)_2(bpy)]^{2+}$.[14] This band and the maximum at 411 nm have also a predominant MLCT character. The offset of the lowest bands between experiment and theory has been observed for other iron complexes, too.[7] Also, the intensities are underestimated in that range. The origin of this problem is currently not clear.[20] For both complexes, the lowest adiabatic triplet state has MC character with energies of 1.31 eV (946 nm) for **Fe1** and 1.62 eV (765 nm) for **Fe2**. Both energies are sufficient for effective oxygen quenching.[24] The excitation from the ground state (^{1}GS) to the lowest triplet states is accompanied by elongation of the central Fe–N bonds by 0.16 Å (**Fe1**) and by 0.28 Å (**Fe2**).[14]

The cyclic voltammogram of **Fe1** shows a reversible wave at 0.74 V (Fig. 2, all redox potentials are given *vs.* FcH/FcH^+) which is assigned to the $Fe^{III/II}$ couple.[7,13] The shift to more anodic potentials compared to $[Fe(tpy)_2]^{2+}$ (0.72 V)[13] indicates a slightly reduced HOMO energy. The HOMO in **Fe1** has a d_π(Fe) character. This points to a similar π-acceptability of the triazoles in

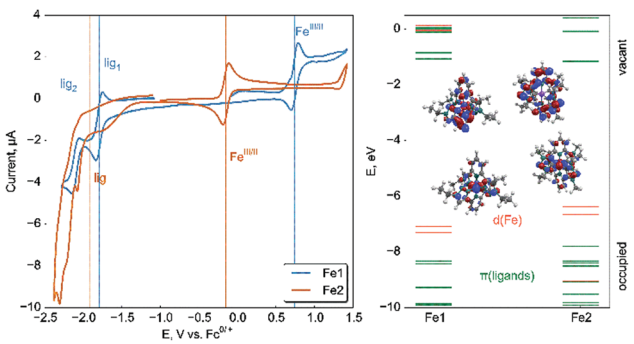

Fig. 2 Cyclic voltammetry (left) and molecular orbital scheme (right) of **Fe1** and **Fe2** including shapes of HOMOs (predominantly localized on *d*(Fe)) and LUMOs (π*-orbitals of ligands).

comparison to tpy. At cathodic potentials, two reversible reductions at −1.79 V and −2.11 V are detected. In analogy to $[Fe(tpy)_2]^{2+}$, they are assigned to a stepwise reduction of the two ligands.[13] The electrochemical energy gap of 2.85 eV (435 nm) is in line with the absorption maximum in the MLCT region.

The $Fe^{III/II}$ couple in **Fe2** is found at a low cathodic potential of −0.15 V. This significant shift in comparison to **Fe1** and $[Fe(bim)_2]^{2+}$ (0.34 V) is intimately connected to the MIC coordination and agrees with reported trends.[7,13] In $[Fe(btz)_2(bpy)]^{2+}$, the $Fe^{III/II}$ couple occurs at a more cathodic potential (−0.35 V). The HOMO of **Fe2** has a dominating d_π(Fe) character and is destabilized by a weaker π-acceptability of the triazolylidenes in comparison to the triazoles. In comparison to imidazolylidene ligands in $[Fe(bim)_2]^{2+}$, the triazolylidine ligands in **Fe2** might have a better π-acceptability,[10,14] as the irreversible reduction in **Fe2** occurs at a potential of −1.91 V.[7] The electrochemical energy gap of 2.00 eV (600 nm) again proves the MLCT assignment of the 593 nm absorption (see Table 1). Electrochemical experiments allow to identify the charge-transfer excited states in **Fe1** and **Fe2**.[22]

These states are probed by ultrafast pump–probe spectroscopy. For **Fe1**, a step-like absorption change at time zero is observed, which persists beyond the experimental time window of 1.6 ns (see Fig. 3A). The transient absorption (TA) spectra reflect the ground state bleach (GSB) but deviate significantly from what is expected for a populated charge transfer state (Fig. 3A, **Fe1**$^+$**–Fe1**).[22] Beside the dominant GSB signature, excited state absorption (ESA) should be detected, which is missing in the TA spectra.

This and the very long lifetime of the TA signal indicate that excitation of **Fe1** results in an ultrafast population of a ligand field MC state. Similar findings related to $^{3/5}MC \rightarrow {}^1GS$ ground state recovery were also reported for other $[FeN_6]^{2+}$ complexes.[5] If the ligand π–π* transitions at 295 nm are excited, **Fe1** exhibits a ligand-based emission at λ_{em} = 334 nm (ΔE_{photon} = 0.49 eV) with a lifetime of τ_{em} = 2.9 ns. Such an emission is not observed in **Fe2**. The TA of **Fe2** is dominated by GSB causing a strong negative band around 600 nm and a less intense one around 420 nm (Fig. 3B). In addition, two ESA features at about 455 nm and in the red spectral region are observed. The TA disappears in less than 50 ps with an evolution, which has to be described by four exponential decay components. One component of 5 fs is an artefact at time zero. The component with a time constant of τ_1 = 0.1 ps is slightly red-shifted compared to the longer living contributions, suggesting an ultrafast relaxation like

Table 1 Physicochemical properties of **Fe1** and **Fe2**

	UV [nm] (ε [M^{-1} cm^{-1}])	CV [V *vs.* FcH/FcH^+]	$\Delta E_{1/2}$	TA	Emission
Fe1	444 (11.500) 295 (44.900)	0.74 (rev.) −1.79 (rev.) −2.11 (rev.)	2.85 eV (435 nm)	$\tau_1 \gg 1.6$ ns	334 nm 2.9 ns
Fe2	593 (21.000) 411 (11.200) 326 (32.500)	−0.15 (rev.) −1.91 (irrev.) −2.15 (irrev.)	1.76 eV (425 nm) 2.00 eV (619 nm)	τ_1 = 0.1 ps τ_2 = 2.7 ps τ_3 = 8.7 ps	—

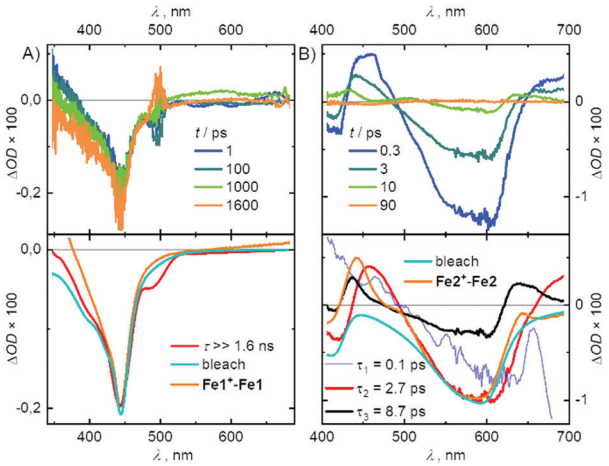

Fig. 3 TA spectra (top) and DAS (bottom) of (A) **Fe1** and (B) **Fe2**. Excited-state differential spectra (orange) approximated as suggested by McCusker *et al.*[22] DAS of **Fe1** was smoothed. Both bleaches and difference spectra were scaled.

vibrational redistribution or intersystem crossing (ISC). The decay associated spectra (DAS) of the dominating component with τ_2 = 2.7 ps and the weaker one with τ_3 = 8.7 ps consist both of the described GSB and ESA features in the blue and red of the GSB, most probably a ^{3}MLCT feature.[14] This conclusion is supported by the difference spectrum of **Fe2**$^+$**–Fe2**, which reproduces the ESA in the blue and the GSB of the two decay components very well. In contrast, the ESA in the red is only insufficiently reflected. This may result from the fact, that for a better description of the MLCT spectrum the difference **Fe2**$^+$ + **Fe2**$^-$**–Fe2** should be considered,[22] which is impossible due to the irreversible ligand reduction.

Analogous behaviour is observed in $[Fe(btz)_2(bpy)]^{2+}$ and the spectral components were assigned to multiple MLCT states.[14] The analysis of data from time-resolved X-ray spectroscopy on this tris(bidentate) reference associated the time constants to different transitions in a hot branching scenario.[23] Transferred to **Fe2** this means a vibrationally hot ^{3}MLCT state is populated by the ultrafast ISC and vibrational redistribution leads within 0.1 ps to a relaxed ^{3}MLCT state. In case of hot branching, the redistribution process competes with a direct channel to the ^{3}MC state in which a large fraction of the population ends up within the first 0.1 ps. The remaining population in the relaxed ^{3}MLCT state decays comparatively slowly (8.7 ps) to the ^{3}MC state, which deactivates more rapidly (2.7 ps) back to the ^{1}GS. In iron carbene complexes the ^{5}MC state are bypassed in the relaxation cascade as strong structural rearrangement is necessary.[4,7] This relaxation scenario is supported by the observation that the DAS of both, the 2.7 ps and the 8.7 ps component exhibit a strong GSB contribution. Although it is not in line with the current literature reports on similar complexes, the following second scenario could also explain the reported findings. The ^{3}MLCT state exhibits two parallel relaxation channels, one leading directly back to the ^{1}GS and the second one to the ^{3}MC state. Then the 2.7 ps have to be assigned to the ^{3}MLCT state and the 8.7 ps to the ^{3}MC state.

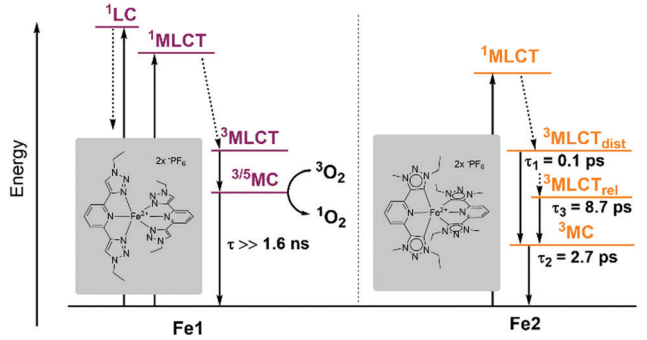

Fig. 4 Proposed relaxation cascade following MLCT excitation of **Fe1** resulting from the experimental findings and of **Fe2** according to the hot branching scenario by Wärnmark *et al.*[14,23]

Further insights into the presence of long-lived triplet states is gained by $^1O_2$ sensitization experiments (see ESI‡).[24] **Fe2** does not show any sensitization activity. In contrast, **Fe1** sensitizes oxygen efficiently after excitation with 480 nm and 275 nm as deduced from energy transfer reaction of formed $^1O_2$ with 1,3-diphenyl-isobenzofuran and detection of the $^1O_2$ emission signal at 1270 nm. A significant ^{3}MC contribution to the relaxation pathway is thus concluded by energy transfer experiments and lowest triplet state optimization, although a ^{5}MC contribution cannot be fully ruled out. McCusker *et al.* recently reported spectroscopical evidence of ^{5}MC states taking part in electron transfer reactions[25] and reactivity of MC-states is also known in chromium(III)- and cobalt(III) complexes.[26,27] The deduced relaxation cascades for **Fe1** and **Fe2** are compared in Fig. 4.

A pair of two pseudo-constitutional Fe^{II} complex isomers with the same ligand core motif, but in form of a triazole $[Fe(N\^N\^N)_2]^{2+}$ (N^N^N = 2,6-bis(1-ethyl-1*H*-1,2,3-triazol-4-yl)pyridine) (**Fe1**) and of a pyridine-MIC $[Fe(C\^N\^C)_2]^{2+}$ (C^N^C = 2,6-bis(1-ethyl-2,3-triazol-5-ylidene)pyridine) (**Fe2**) is presented. **Fe1** shows a similar excited state behaviour as other $[Fe(N\^N\^N)_2]^{2+}$ complexes, such as $[Fe(tpy)_2]^{2+}$ with a long-lived ^{3}MC, identified by its transient absorption and $^1O_2$ sensitizing activity. This bis(triazolyl)pyridine complex offers thus a potential new class of Fe^{II} complexes that enable energy transfer reactions by excitation, making use of metal centred states. Despite a significantly reduced octahedral symmetry, the bis(tridentate) $[Fe(C\^N\^C)_2]^{2+}$ complex **Fe2** shows a very similar behaviour as the tris(bidentate) $[Fe(C\^C)_2(N\^N)]^{2+}$ complex $[Fe(btz)_2(bpy)]^{2+}$. Transient absorption of **Fe2** suggests analogous hot branching dynamics as in $[Fe(btz)_2(bpy)]^{2+}$. Comparing the photophysics of tetra-MIC **Fe2** and $[Fe(btz)_2(bpy)]^{2+}$ – which show both a net coordination of two nitrogen and four carbon ligand atoms – the bis(tridentate) $[Fe(C\^N\^C)_2]^{2+}$ form appears to be equivalent or even slightly superior to the tris(bidentate) $[Fe(C\^C)_2(N\^N)]^{2+}$ in terms of excited state lifetimes.

Financial support from the Deutsche Forschungsgemeinschaft [DFG, Priority Program SPP 2102] ''Light-controlled reactivity of metal complexes'' (BA 4467/7-1, LO 714/11-1, KU 952/12-1, SE 1448/8-1, HE 2778/14-1) is gratefully acknowledged by M. B., O. K., S. L., M. S. and K. H. P. D. thanks the Fonds der Chemischen Industrie for a Kekulé grant. O. B. thanks Grant No. 14.Y26.31.0019 from Ministry of Education and Science of Russian Federation for financial support.

Conflicts of interest

There are no conflicts to declare.

References

1 V. Balzani, G. Bergamini, S. Campagna and F. Puntoriero, *Photochemistry and Photophysics of Coordination Compounds I*, Springer, 2007, pp. 1–36.
2 C. Förster and K. Heinze, *Chem. Soc. Rev.*, 2020, **49**, 1057.
3 O. S. Wenger, *Chem. – Eur. J.*, 2019, **25**, 6043.
4 Y. Liu, P. Persson, V. Sundström and K. Wärnmark, *Acc. Chem. Res.*, 2016, **49**, 1477.
5 L. L. Jamula, A. M. Brown, D. Guo and J. K. McCusker, *Inorg. Chem.*, 2014, **53**, 15.
6 A. K. C. Mengel, C. Förster, A. Breivogel, K. Mack, J. R. Ochsmann, F. Laquai, V. Ksenofontov and K. Heinze, *Chem. – Eur. J.*, 2015, **21**, 704.
7 P. Dierks, A. Päpcke, O. S. Bokareva, B. Altenburger, T. Reuter, K. Heinze, O. Kühn, S. Lochbrunner and M. Bauer, *Inorg. Chem.*, 2020, **59**, 14746.
8 Y. Liu, T. Harlang, S. E. Canton, P. Chábera, K. Suárez-Alcántara, A. Fleckhaus, D. A. Vithanage, E. Göransson, A. Corani, R. Lomoth, V. Sundström and K. Wärnmark, *Chem. Commun.*, 2013, **49**, 6412.
9 P. Chábera, K. S. Kjaer, O. Prakash, A. Honarfar, Y. Liu, L. A. Fredin, T. C. B. Harlang, S. Lidin, J. Uhlig, V. Sundström, R. Lomoth, P. Persson and K. Wärnmark, *J. Phys. Chem. Lett.*, 2018, **9**, 459.
10 D. G. Brown, N. Sanguantrakun, B. Schulze, U. S. Schubert and C. P. Berlinguette, *J. Am. Chem. Soc.*, 2012, **134**, 12354.
11 J. Beerhues, H. Aberhan, T.-N. Streit and B. Sarkar, *Organometallics*, 2020, **39**, 4557.
12 D. Schweinfurth, L. Hettmanczyk, L. Suntrup and B. Sarkar, *Z. Anorg. Allg. Chem.*, 2017, **643**, 554.
13 P. Zimmer, L. Burkhardt, A. Friedrich, J. Steube, A. Neuba, R. Schepper, P. Müller, U. Flörke, M. Huber, S. Lochbrunner and M. Bauer, *Inorg. Chem.*, 2018, **57**, 360.
14 Y. Liu, K. S. Kjaer, L. A. Fredin, P. Chábera, T. Harlang, S. E. Canton, S. Lidin, J. Zhang, R. Lomoth, K.-E. Bergquist, P. Persson, K. Wärnmark and V. Sundström, *Chem. – Eur. J.*, 2015, **21**, 3628.
15 M. Ostermeier, M.-A. Berlin, R. M. Meudtner, S. Demeshko, F. Meyer, C. Limberg and S. Hecht, *Chem. – Eur. J.*, 2010, **16**, 10202.
16 D. Schweinfurth, S. Demeshko, S. Hohloch, M. Steinmetz, J. G. Brandenburg, S. Dechert, F. Meyer, S. Grimme and B. Sarkar, *Inorg. Chem.*, 2014, **53**, 8203.
17 H. Oshio, H. Spiering, V. Ksenofontov, F. Renz and P. Gütlich, *Inorg. Chem.*, 2001, **40**, 1143.
18 H. Iwasaki, Y. Koga and K. Matsubara, *Org. Chem.: Curr. Res.*, 2016, **5**, 161.
19 T. Möhle, O. S. Bokareva, G. Grell, O. Kühn and S. I. Bokarev, *J. Chem. Theory Comput.*, 2018, **14**, 5870.
20 O. S. Bokareva, O. Baig, M. J. Al-Marri, O. Kühn and L. González, *Phys. Chem. Chem. Phys.*, 2020, **22**, 27605.
21 F. Plasser, *J. Chem. Phys.*, 2020, **152**, 84108.
22 A. M. Brown, C. E. McCusker and J. K. McCusker, *Dalton Trans.*, 2014, **43**, 17635.
23 H. Tatsuno, *et al.*, *Angew. Chem., Int. Ed.*, 2020, **59**, 364.
24 C. Schweitzer and R. Schmidt, *Chem. Rev.*, 2003, **103**, 1685.
25 M. D. Woodhouse and J. K. McCusker, *J. Am. Chem. Soc.*, 2020, **142**, 16229.
26 S. Otto, M. Dorn, C. Förster, M. Bauer, M. Seitz and K. Heinze, *Coord. Chem. Rev.*, 2018, **359**, 102.
27 S. Kaufholt, N. W. Rosemann, P. Chábera, L. Lindh, I. Bolaño Losada, J. Uhlig, T. Pascher, D. Strand, K. Wärnmark, A. Yartsev and P. Persson, *J. Am. Chem. Soc.*, 2021, **143**, 1307.